

NEARBY GROUPS OF GALAXIES IN THE HERCULES–BOOTES CONSTELLATIONS

I. D. Karachentsev^{1, (*)}, O. G. Kashibadze¹, V. E. Karachentseva²

¹*Special Astrophysical Observatory of Russian AS, Nizhnij Arkhiz 369167, Russia*

²*Main Astronomical Observatory, National Academy of Sciences of Ukraine, Kiev, 03143 Ukraine*

(Received March 2, 2017; Revised March 17, 2017)

We consider a sample of 412 galaxies with radial velocities $V_{\text{LG}} < 2500 \text{ km s}^{-1}$ situated in the sky region of $\text{RA} = 13^{\text{h}}0\text{--}19^{\text{h}}0$, $\text{Dec} = +10^\circ \dots +40^\circ$ between the Local Void and the Supergalactic plane. One hundred and eighty-one of them have individual distance estimates. Peculiar velocities of the galaxies as a function of Supergalactic latitude SGB show signs of Virgocentric infall at $SGB < 10^\circ$ and motion from the Local Void at $SGB > 60^\circ$. A half of the Hercules–Bootes galaxies belong to 17 groups and 29 pairs, with the richest group around NGC 5353. A typical group is characterized by the velocity dispersion of 67 km s^{-1} , the harmonic radius of 182 kpc, the stellar mass of $4.3 \times 10^{10} M_\odot$ and the virial-to-stellar mass ratio of 32. The binary galaxies have the mean radial velocity difference of 37 km s^{-1} , the projected separation of 96 kpc, the mean integral stellar mass of $2.6 \times 10^9 M_\odot$ and the mean virial-to-stellar mass ratio of about 8. The total dark-matter-to-stellar mass ratio in the considered sky region amounts to 37 being almost the same as that in the Local Volume.

Keywords: galaxies: kinematics and dynamics—galaxies: distances and redshifts—galaxies: groups

1 Introduction

Mass radial-velocity measurements of galaxies in the recent optical and radio sky surveys like the SDSS [1], HIPASS [2, 3, 4], and ALFALFA [5, 6] led to a significant enrichment in our understanding of the large-scale structure and galaxy motions in the nearby universe. Based on the data on approximately 10^4 galaxies with radial velocities relative to the centroid of the Local Group $V_{\text{LG}} < 3500 \text{ km s}^{-1}$, Karachentsev and Makarov [7, 8, 9] compiled catalogs of galaxy systems of different multiplicity throughout the sky, with the total number of about a thousand. For galaxy clustering, a new algorithm was applied that took into account individual masses (luminosities) of galaxies. Using the mutual separations, radial velocities and luminosities of galaxies in the K -band, they determined virial and stellar masses of galaxy systems in the volume of a 48 Mpc radius, which covers the entire Local Supercluster and its nearest neighborhood.

One of important results of these studies was the estimation of the bulk matter density, enclosed in the systems of galaxies, $\Omega_m^{\text{vir}} = 0.08 \pm 0.02$, which proved to be 3 to 4 times lower than the average global matter density $\Omega_m = 0.26 \pm 0.02$ [10]. Various assumptions were made to explain this discrepancy, listed in [11]:

a) groups and clusters are surrounded by extended dark haloes, and their main dark mass is localized outside the

virial radius of the system;

b) the considered volume of the Local Universe is not representative, being located in a giant cosmic void;

c) a large part of dark matter in the universe is not enclosed in groups and clusters, but is distributed between them in diffuse large-scale structures (filaments, knots).

However, none of these assumptions has yet received any convincing observational evidence. Further accumulation of data on the radial velocities and distances of galaxies is obviously required, as well as the verification of the effectiveness of the criterium unifying the galaxies into groups. Following this idea, we conducted an analysis of observational data on galaxies in 5 areas with a fairly representative number of objects. Three of them are located along the plane of the Local Supercluster to the north [12, 13] and to the south [14] from the Virgo cluster. Two other: the Bootes region [15] and the Leo–Cancer region [16] cover the zones at high supergalactic latitudes. Location of the studied sky regions is demonstrated in Fig. 1 in equatorial coordinates. Points mark the positions of 5725 galaxies with radial velocities of $V_{\text{LG}} < 3000 \text{ km s}^{-1}$, a ragged ring-shaped band denotes a zone of strong extinction in the Milky Way. In addition to the 5 previous zones (marked in a light gray tone), we are considering here a new region, bounded by the following coordinates: RA from $13^{\text{h}}0$ to $19^{\text{h}}0$, and Dec from $+10^\circ$ to

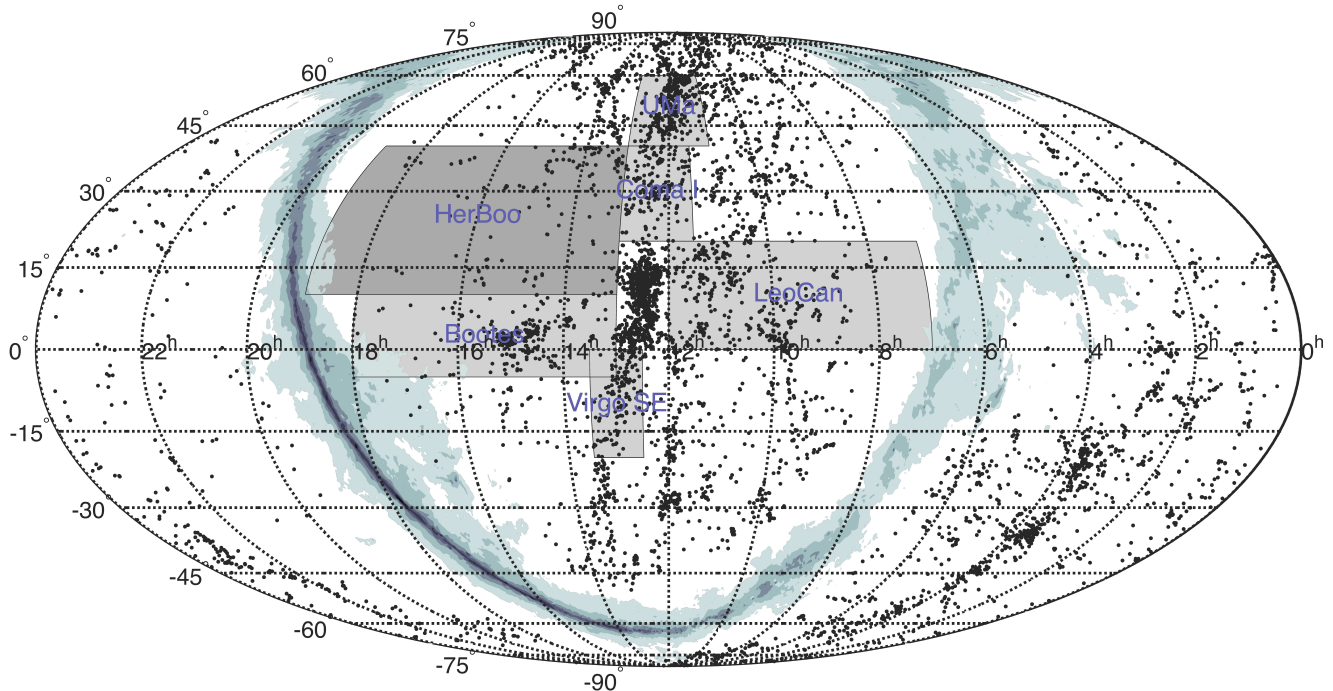


Figure 1: Sky distribution of the Local Supercluster galaxies in equatorial coordinates. The Hercules–Bootes and five other regions we have previously studied are marked in dark color. A ring-shaped patchy band indicates a zone of strong extinction.

+40°. Since the relative number of galaxies with distance estimates steeply drops with increasing radial velocity of galaxies, we confined ourselves to considering only the objects with the velocities of $V_{LG} < 2500 \text{ km s}^{-1}$, which corresponds to a somewhat larger volume than those in our previous studies.

2 Observational data

The region in question partially overlaps with the SDSS, HIPASS and ALFALFA sky survey regions. The main source of galaxy data we used is the NASA Extragalactic Database (NED)^(**) with additions from the HyperLEDA [17]. Each object with a radial velocity estimate V_h was visually inspected, and a large number of false ‘galaxies’ with radial velocities of around zero was discarded. For many galaxies, we have refined the morphological types and integral B -magnitudes. In the absence of photometric data the apparent magnitudes of a number of galaxies, usually dwarf ones, were estimated comparing them with the images of other objects having a similar structure and reliable photometry.

In total, there are 412 galaxies in this region of the sky possessing radial velocities of $V_{LG} \leq 2500 \text{ km s}^{-1}$. Their list is presented in Table 1, the full version of which is avail-

able in the electronic form in the Vizier database^(***). The columns of the table contain: (1) the name of the galaxy or its number in well-known catalogs; (2) equatorial coordinates for the epoch (2000.0); (3) radial velocity (in km s^{-1}) relative to the centroid of the Local Group with the apex parameters accepted in the NED; (4) morphological type of the galaxy according to the de Vaucouleurs classification; (5) integral apparent magnitude of the galaxy in the B -band; (6) the FWHM of the 21 cm radio line (in km s^{-1}); (7) the distance modulus corrected for the extinction in the Galaxy [18] and internal extinction [19]; (8) the method by which the distance modulus is determined; (9) the name of the brightest galaxy in the group/pair to which this galaxy belongs according to [8, 9] or [7].

The considered region of the sky contains only one galaxy with a high-accuracy measurement of distance by the cepheids (“cep”). For four early-type galaxies the distances are determined by the surface brightness fluctuations (“sbf”, [20]), and for nine very nearby galaxies the distances are measured by the luminosity of the red giant branch (“rgb”). In the remaining galaxies of our sample the distance moduli are determined by the Tully–Fisher relationship [21] with the calibration according to [22]:

^(***)<http://cdsarc.u-strasbg.fr/viz-bin/qcat?J/other/AstBu/72.2>

^(**)<http://ned.ipac.caltech.edu>

Table 1: Galaxies in the Hercules–Bootes region

Name	RA (2000.0) Dec	V_{LG}	T	B_T	W_{50}	$(m - M)$	Method	Group
(1)	(2)	(3)	(4)	(5)	(6)	(7)	(8)	(9)
UGC 8085	125817.3+143325	1971	Scd	14.5	204	32.37	tf	N 4866
NGC 4866	125927.1+141016	1911	Sb	12.14	514	32.21	tf	N 4866
NGC 4880	130010.6+122900	1293	S0a	13.12				
AGC 233925	130015.7+292859	2482	dIr	18.08	90			
AGC 239030	130018.9+293305	970	dIr	18.7	40	31.57	bTF	
AGC 233574	130022.1+125525	1838	dIr	17.6	70	32.74	TF	N 4866
UGC 08114	130025.0+134013	1909	Sm	15.85	130	32.91	TF	N 4866
PGC 1876816	130242.8+294458	2520	dIm	18.30				
AGC 732482	130336.8+243132	816	Sm	16.2	97	32.15	TF	
AGC 233930 *	130402.7+281833	674	dIm	17.17	98			
KK 181	130433.8+264627	1916	dIr	16.88	86	32.74	TF	
KUG 1302+329	130439.4+324054	2372	BCD	16.6				
SDSS J130440	130440.0+184439	766	BCD	17.73				
IC 4171	130518.8+360610	1026	Sdm	15.9	89	31.73	TF	
UGC 08181	130524.6+325400	900	Sdm	15.59	84	31.30	TF	
IC 4178	130541.5+360103	1215	dIm	16.53	64	31.48	TF	
NGC 4961	130547.6+274400	2525	Scd	13.7	216	33.00	tf	N 4961
IC 4182	130549.6+373618	357	Sm	12.00	35	28.36	cep	N 4736
BTS 165	130549.8+274240	2516	dIr	17.0				N4961
AGC 230077	130623.3+102600	841	dIm	15.66	46	30.79	TF	
KK 183	130642.5+180008	1496	dIr	17.90	75	31.98	bTF	
AGC 230084	130656.0+144826	915	dIm	16.39	49	30.40	TF	
PGC 2134801	130717.2+384321	2423	dIm	17.1				
AGC 239031	130812.3+290517	822	dIr	18.3	23	29.96	TF	
AGC 742775 *	130828.4+200202	1430	dIr	18.2	146			
PGC 1958740	130936.9+314034	1449	BCD	17.8				
AGC 742788 *	131000.8+185530	2365	BCD	18.1	157			
UGC 08246	131004.9+341051	825	SBc	14.82	116	30.90	tf	U 8246
2MFGC 10495	131024.2+213434	2547	Sc	16.28				
[MU 2012] J13	131029.2+341413	873	dIm	17.4				U 8246
NGC 5002	131038.2+363804	1125	Sm	14.69	90	30.42	tf	N 5005
PGC 2089756	131051.1+365623	1061	dIr	17.8				
NGC 5005	131056.3+370333	983	Sb	10.54	490	31.54	tf	N 5005
UGC 08261	131101.0+353008	881	Sm	16.36	94	31.70	bTF	N 5005
SDSS J131115	131115.8+365912	992	dIr	18.43				
PGC 2097739	131126.8+371843	998	dIm	17.48				

$$M_B = -7.27(\log W_{50}^c - 2.5) - 19.99,$$

where M_B is the absolute magnitude in the B -band, and the width of the HI line (in km s^{-1}) is corrected for the inclination of the galaxy. These estimates are denoted in Table 1 as “TF”. For late-type galaxies (dIr, dIm, Sm) in which the HI-value $m_{21} = -2.5 \log F(\text{HI}) + 17.4$ is brighter than the apparent magnitude, $m_{21} < B$, we introduced the “baryon correction”, replacing the B -magnitude in the distance modulus by m_{21} . We designated these cases as “bTF”. Galaxies with the average distance modulus values from the NED are marked in column (8) by lower-case letters “tf”. In total in the region considered, there are 167 galaxies with distance estimates by Tully–Fisher, among them our new estimates make up about 70%.

In some galaxies from the ALFALFA HI-survey [5, 6] the width of the W_{50} radio line does not correspond to the structural type of the galaxy T and its apparent magnitude B_T . The reason for this discrepancy may be a confusion during the optical identification of a radio source, or a low signal-to-noise ratio in the HI line. Such galaxies are marked in Table 1 with an asterisk.

The distribution of 412 galaxies by radial velocity and 181 galaxies by the distance are shown in Figs. 2a, b, respectively. Several galaxies with velocities greater than 2500 km s^{-1} belong to the NGC 5353 and NGC 6181 group members, the average velocity of which lies at the boundary of the selected range V_{LG} . Figure 2a reveals a local excess of galaxies with the velocities of about 1000 km s^{-1} , which is obviously due to the presence of galaxies, associated with the spurs of the Virgo cluster in the considered region. A part of these galaxies apparently causes a peak that is noticeable in the $N(D)$ distribution at the distance of $D \simeq 18 \text{ Mpc}$ (Fig. 2b).

Figure 2c reproduces the distribution of 181 Hercules–Bootes galaxies throughout the peculiar velocity $V_{\text{pec}} = V_{\text{LG}} - H_0 \times D$, given the value of the Hubble parameter of $H_0 = 73 \text{ km s}^{-1} \text{ Mpc}^{-1}$. The histogram has a completely symmetrical shape with the average value of $V_{\text{pec}} = -179 \text{ km s}^{-1}$ and the variance of 425 km s^{-1} . With an average distance of the sample galaxies of about 26 Mpc and a typical distance error of around 20%, the expected accuracy of peculiar velocity is 380 km s^{-1} . The excess of the observed velocity dispersion over the expected dispersion may indicate the existence of large-scale motions of galaxies in the Hercules–Bootes region. Note that in the volume we consider, the number of galaxies with peculiar velocity estimates is approximately twice as large as that contained in the Cosmicflows-2 and Cosmicflows-3 databases of galaxy distances [23, 24].

The total distribution of 412 Hercules–Bootes galax-

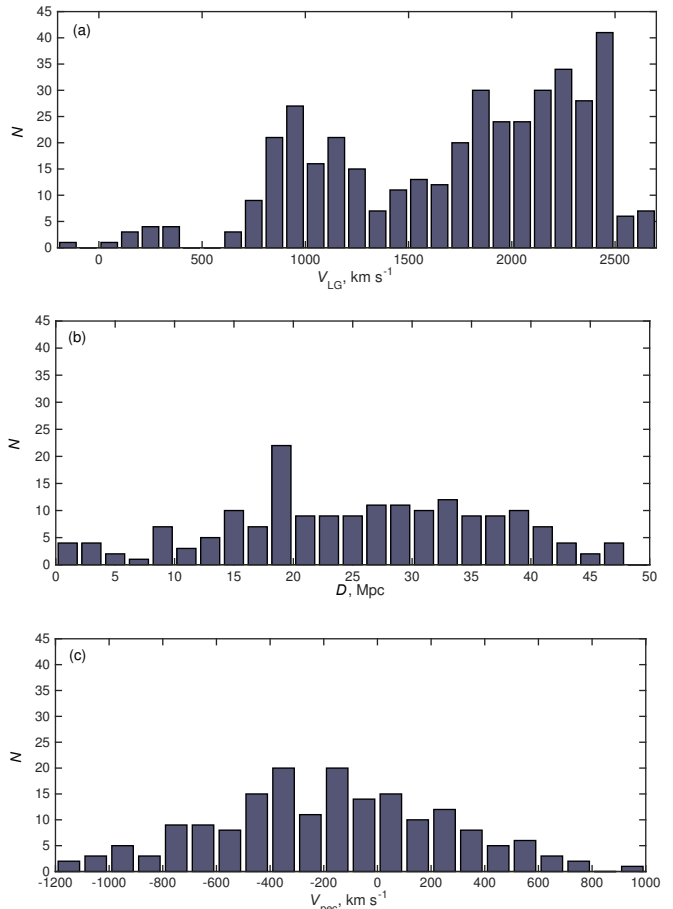


Figure 2: The distribution of the number of galaxies in the Hercules–Bootes region based on (a) radial velocities relative to the centroid of the Local Group, (b) distances and (c) peculiar velocities.

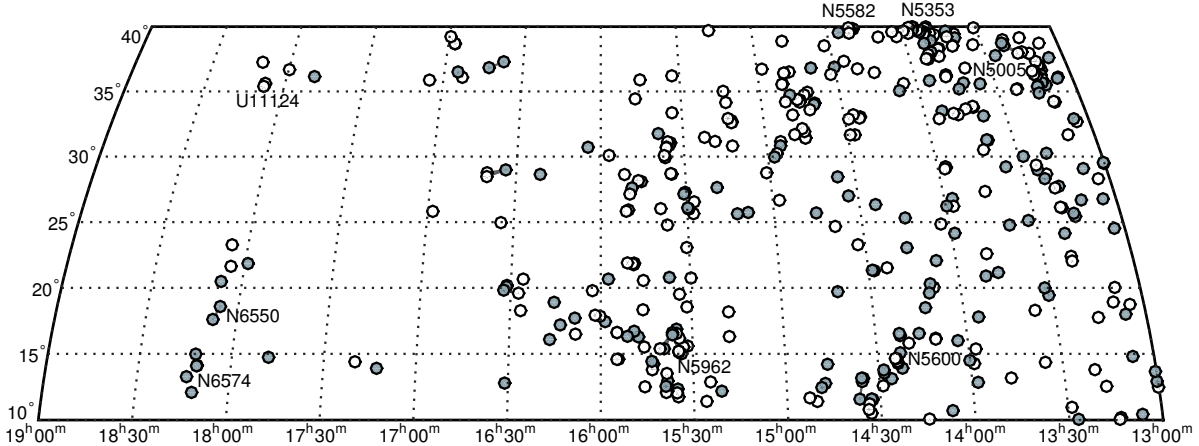


Figure 3: The distribution of galaxies in the Hercules–Bootes region in equatorial coordinates. Galaxies with distance estimates are represented by filled circles, the remaining galaxies with velocities of $V_{LG} < 2500 \text{ km s}^{-1}$ are shown by open circles. The brightest members of some groups are marked with their names.

ies in equatorial coordinates is shown in Fig. 3. Galaxies with distance estimates and without them are marked by dark and bright circles, respectively. The most populated groups are designated by the names of their brightest members. This diagram demonstrates the clustering of galaxies into systems of different multiplicity, as well as a global increase in the number density of galaxies from the left to the right edge approaching the equator of the Local Supercluster.

3 Groups and pairs of galaxies

Combining the galaxies into systems of different multiplicity, we were guided by the criterion proposed in the paper [9]. According to it, each virtual pair ij must satisfy the condition of negative total energy

$$V_{ij}^2 R_{ij} / (2GM_{ij}) < 1,$$

where G is the gravity constant, and the condition of finding its components inside the “zero-velocity sphere”, which isolates this pair relative to the global Hubble expansion

$$\pi H_0^2 R_{ij}^3 / (8GM_{ij}) < 1,$$

where H_0 is the Hubble parameter. Here V_{ij} and R_{ij} are the differences between the radial velocities and the projection of mutual separations of the virtual pair components, M_{ij} is their total mass expressed through the K -luminosity $M/L_K = \kappa M_\odot / L_\odot$. To estimate the total mass of the galaxy, we took the value of the dimensionless parameter $\kappa = 6$, at which the structure and virial mass of the well-studied nearby groups is best reproduced. The clustering algorithm involves a sequential revision of

all the galaxies of the initial selection and the subsequent grouping of all pairs possessing common members.

Therefore, 17 galaxy groups with populations of three or more members were selected in the considered region of the sky. The main data about them are presented in the columns of Table 2: (1) the name of the brightest member of the group; (2) the equatorial coordinates of the center of the group; (3) the number of members with measured radial velocities; (4) the average radial velocity of the group (km s^{-1}); (5) the root-mean-square velocity of galaxies relative to the average (km s^{-1}); (6) the harmonic average radius of the group (kpc); (7) the logarithm of the total stellar mass of the group (in M_\odot units), determined from the K -band luminosity of its members at $M^*/L_K = M_\odot / L_\odot$; (8) the logarithm of the projected (virial) mass in M_\odot units:

$$M_p = (32/\pi G)(N - 3/2)^{-1} \sum_{i=1}^N \Delta V_i^2 R_i,$$

where ΔV_i and R_i are the radial velocity and the projection distance of the i -th galaxy relative to the center of the system; (9) the number of members with measured distances; (10) the average distance modulus of the group; (11) the variance of the moduli of the group members; (12) linear distance in Mpc at the mean modulus $\langle m - M \rangle$; (13) peculiar velocity of the center of the group, $V_{pec} = \langle V_{LG} \rangle - 73 \langle D \rangle$, (km s^{-1}). The last row of the table corresponds to the average values of the parameters.

As follows from these data, the characteristic radius of the group (182 kpc) and the characteristic dispersion of radial velocities (67 km s^{-1}) prove to be typical of the Local Group and other nearby groups in the Local Volume [25]. The characteristic stellar mass of the group in

Table 2: Properties of the galaxy groups in the Hercules–Bootes region

Group	J2000.0	N_V	$\langle V_{LG} \rangle$	σ_V	R_h	$\log M^*$	$\lg M_p$	N_D	$\langle m - M \rangle$	$\sigma(m - M)$	D	V_{pec}
(1)	(2)	(3)	(4)	(5)	(6)	(7)	(8)	(9)	(10)	(11)	(12)	(13)
NGC 4736	125053.1+410714	13	352	50	338	10.64	12.33	13	28.28	0.14	4.5	24
NGC 4866	125927.1+141016	5	1909	58	156	11.21	12.68	4	32.56	0.28	32.5	−464
NGC 5005	131056.2+370333	13	1010	114	224	11.48	12.97	9	31.24	0.41	17.7	−282
NGC 5117	132256.4+281859	4	2414	27	424	9.97	11.95	2	32.80	0.09	36.3	−236
NGC 5353	135539.9+402742	62	2593	195	455	12.07	13.69	16	32.73	0.39	35.2	16
NGC 5375	135656.0+290952	3	2311	47	66	10.62	11.68	1	32.94	–	38.7	−514
NGC 5582	142043.1+394137	6	1685	106	93	10.60	12.44	2	31.82	0.54	23.1	−1
NGC 5600	142349.5+143819	6	2295	81	275	10.69	12.38	3	32.05	0.91	25.7	419
UGC 9389	143533.2+125429	4	1822	45	204	9.68	12.08	4	32.54	0.19	32.2	−529
PGC 55227	152929.2+260024	3	2119	14	17	9.21	10.05	2	32.34	0.17	29.4	−27
NGC 5961	153516.2+305152	5	1891	63	86	10.14	12.20	1	32.51	–	31.8	−430
NGC 5962	153631.7+163628	8	1996	97	60	11.23	13.01	6	32.60	0.35	33.1	−420
NGC 5970	153830.0+121110	4	1949	92	141	10.81	12.54	3	32.45	0.28	30.9	−307
UGC 10043	154841.3+215210	5	2214	67	65	10.37	11.88	1	33.03	–	40.4	−735
NGC 6181	163221.0+194936	4	2568	53	196	11.06	12.14	3	32.65	0.19	33.9	93
UGC 10445	163347.4+285904	3	1118	23	230	9.92	11.60	1	31.57	–	20.6	−386
NGC 6574	181151.2+145854	3	2456	15	70	11.08	10.71	2	32.36	0.43	29.6	295
Average		9	1924	67	182	10.63	12.14	4	32.15	0.34	29.2	−205

Table 2, $M^* \simeq 4 \times 10^{10} M_\odot$, and virial-to-stellar mass ratio, $M_p/M^* \simeq 32$, are also typical for the well-studied nearby groups.

If the clustering algorithm for galaxies is correctly selected, then the distance modulus variance of group members should be determined by the distance measurement errors. In our case, the distances of most galaxies are measured by the Tully–Fisher method, the error of which is approximately 20% or 0.4. The average modulus variance for members of 17 groups amounts to 0.34, i.e. it is in agreement with the expected value.

Among the 17 groups listed in Table 2, a group of galaxies around NGC 5353 is distinguished by large stellar and virial masses. The structure and morphological composition of this group were investigated in [26]. From the radial velocities of fifteen brightest members of the group the authors have identified the virial mass of this system as $2.1 \times 10^{13} M_\odot$. Our estimate of the total mass of the NGC 5353 group from 62 galaxies with measured velocities gives a twice higher value. In this case, the $M_p/M^* = 47$ ratio for it also looks typical of rich groups, similar to the nearby group Leo I. Considering the filamentary structures of galaxies in the broad vicinity of the Virgo cluster, Kim et al. [27] suggested that the NGC 5353 group is connected to the Virgo by a long (about 25°) thin filament. However, our data on the velocities and distances of galaxies in this area does not support this assumption.

In addition to 17 groups, this region contains 29 pairs of galaxies, a summary on which is presented in Table 3.

The designations of the columns in it are similar to the previous table. A typical pair has a difference of the component radial velocities of $\langle \Delta V_{12} \rangle = 37 \text{ km s}^{-1}$, the projection distance between the components of $\langle R_{12} \rangle = 96 \text{ kpc}$ and the stellar mass of $\langle \log M^*/M_\odot \rangle = 9.42$. The projected (orbital) mass of the pair,

$$M_p = (16/\pi G)(\Delta V_{12})^2 R_{12}$$

is on the average 8 times the total stellar mass: $\langle \log(M_p/M^*) \rangle = 0.92$. The mean difference of the distance moduli for the components of the pairs, 0.45, testifies to an insignificant share of fictitious optical pairs among them.

Figure 4 shows the Hubble velocity–distance diagram for the centers of groups and pairs of galaxies in the Hercules–Bootes region. Groups with individual distance estimates for two or more members are denoted by solid squares, while the groups with $N_D = 1$ are shown as empty squares. The pairs of galaxies with $N_D = 2$ and $N_D = 1$ are depicted, respectively, by solid and empty triangles. The straight line corresponds to the Hubble parameter of $73 \text{ km s}^{-1} \text{ Mpc}^{-1}$. It is clear from these data that an increase in the number of group members with Tully–Fisher distance estimates favours to reduce dispersion of peculiar velocities in the group centers. We expect that groups of galaxies identified by the criterion [9] with $N_D > 4$ have a typical error of the average distance measurement of about 10%, i.e. their average velocities and average distance estimates by the Tully–Fisher method

Table 3: Pairs of galaxies in the Hercules–Bootes region

Name	$\langle V_{\text{LG}} \rangle$	ΔV	D	R_p	$\log M^*$	$\log M_{\text{orb}}$	$\Delta(m - M)$
(1)	(2)	(3)	(4)	(5)	(6)	(7)	(8)
UGC 8246	849	48	15.1	27	8.48	10.86	–
UGC 8318	2417	18	41.5	56	9.71	10.22	–
AGC 732599	1902	24	26.1	55	8.13	10.57	–
UGC 8507	980	29	12.6	132	9.25	11.11	0.87
PGC 169748	728	13	14.6	77	7.87	10.18	–
UGC 8667	1417	26	19.4	13	8.63	10.02	–
NGC 5303	1473	22	18.7	15	9.81	9.93	–
IC 4341	2386	39	38.4	103	10.06	11.26	–
NGC 5611	2076	80	25.2	54	10.23	11.61	–
UGC 9274	1162	12	15.4	42	8.82	9.85	0.10
IC 1014	1278	2	18.3	73	9.37	8.53	0.43
UGC 9320	864	8	12.6	133	7.08	9.99	–
UGC 9356	2181	56	35.0	61	9.76	11.35	0.96
NGC 5727	1578	4	23.5	55	9.20	9.01	–
UGC 9504	1592	11	21.8	8	8.98	9.05	–
UGC 9519	1711	18	23.4	101	10.00	10.58	–
NGC 5762	1798	7	29.1	218	9.92	10.10	0.32
PGC 2080256	1978	1	27.1	10	8.70	7.07	–
UGC 9562	1334	112	18.3	21	9.19	11.49	–
NGC 5798	1881	24	25.1	152	9.98	11.01	–
AGC 733735	2100	42	38.3	106	8.90	11.34	–
NGC 5958	2119	12	29.0	43	10.17	9.86	–
NGC 5956	1905	70	26.1	143	10.59	11.91	–
NGC 6012	2012	175	21.7	48	10.50	12.24	–
UGC 10086	2378	166	32.6	9	10.18	11.44	–
NGC 6207	1035	4	17.5	360	10.16	9.83	0.28
NGC 6255	1100	23	19.9	194	9.60	11.08	–
UGC 10625	2256	1	33.3	16	9.03	7.27	–
NGC 6550	2410	15	24.2	454	10.85	11.08	0.21
Average	1686	37	24.3	96	9.42	10.34	0.45

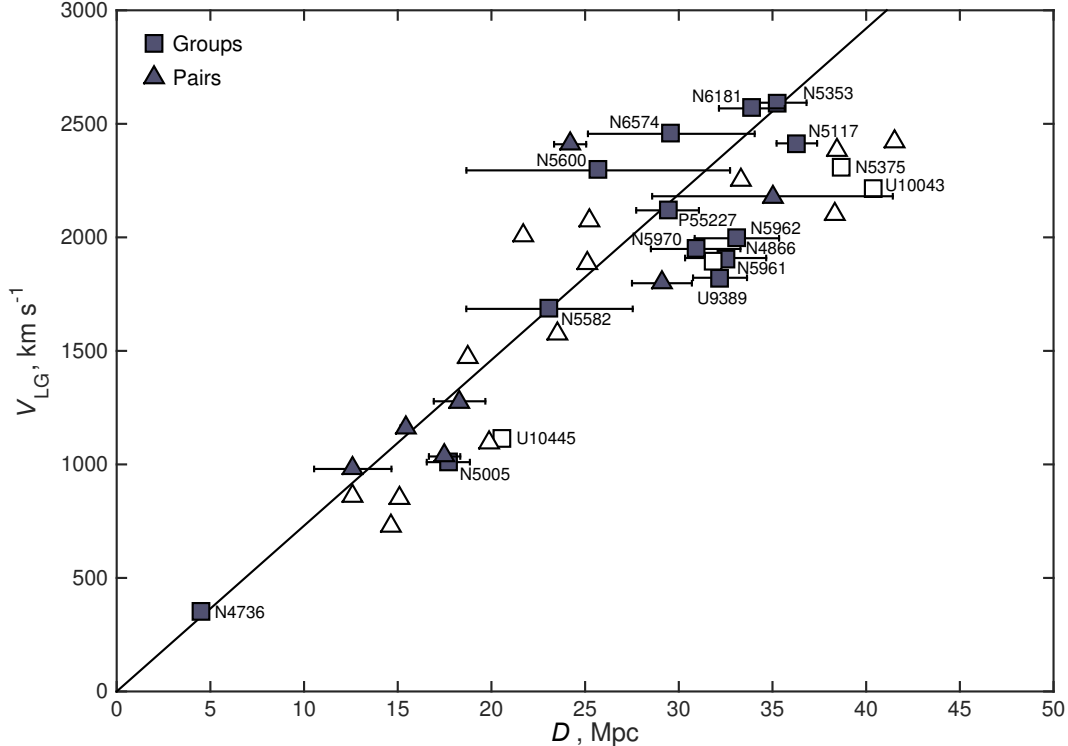


Figure 4: Hubble velocity–distance diagram for group centers (squares) and pairs of galaxies (triangles). Systems with distance estimates for two and more members are indicated by solid symbols with mean errors marked.

can be successfully used for tracing the field of peculiar velocities along with other high-accuracy methods (“cep”, “SN”, “rgb”).

4 Peculiar motions in the Hercules–Bootes region

Considering the observational data on radial velocities and distances of the galaxies in the Local Supercluster and its environs, Tully et al. [28] have identified two main factors, forming the local field of peculiar velocities: the infall of galaxies to the center of the Virgo cluster (the so-called Virgocentric infall) at a characteristic rate of about 180 km s^{-1} and the outflow of galaxies from the center of the expanding Local Void with the typical velocity of about 260 km s^{-1} . It is obvious that both these effects should influence the peculiar velocity field in the Hercules–Bootes region, stretching between the Local Void and the Virgo cluster.

Since the suspected center of the Local Void is located near the northern supergalactic pole at the latitude $\text{SGB} \simeq +77^\circ$ [29], and the center of Virgo is almost on the equator of the Local Supercluster ($\text{SGB} \simeq -2^\circ$), then the approximate orthogonality of these directions facilitates the analysis of the peculiar velocity field between them.

For all the galaxies in the $\text{RA} = [13^{\text{h}}0, 19^{\text{h}}0]$, $\text{Dec} = [+10^\circ, +40^\circ]$ region with the D and V_{pec} estimates we have determined supergalactic coordinates SGL and SGB. To make the picture complete we added 161 galaxy from the Bootes strip to this sample: $\text{RA} = [13^{\text{h}}0, 18^{\text{h}}0]$, $\text{Dec} = [-5^\circ, +10^\circ]$, with radial velocities of $V_{\text{LG}} < 2000 \text{ km s}^{-1}$. The behavior of the median value of peculiar velocity of galaxies along the supergalactic latitude is shown in Fig. 5. The solid broken line corresponds to a running median with an averaging window of 2.5. In order to make the combined sample more homogeneous, we excluded from it the Hercules–Bootes galaxies with $V_{\text{LG}} > 2000 \text{ km s}^{-1}$. The galaxies of the Hercules–Bootes and Bootes strip regions are depicted in the figure by solid and open circles, respectively.

As follows from these data, at intermediate supergalactic latitudes of $\text{SGB} = [+10^\circ, +60^\circ]$ the values of the median peculiar velocity of galaxies vary in a narrow range from -200 to -400 km s^{-1} . At low supergalactic latitudes, $\text{SGB} < 10^\circ$, the median value V_{pec} drops to the minimum value of about -700 km s^{-1} . Most of the galaxies in the $\text{SGB} < 10^\circ$ zone have the distances of $D > 16 \text{ Mpc}$, i.e. they are behind the Virgo cluster. Falling in the direction of the Virgo cluster as a massive local attractor, these galaxies acquire a significant negative line of sight peculiar velocity. The observed amplitude of

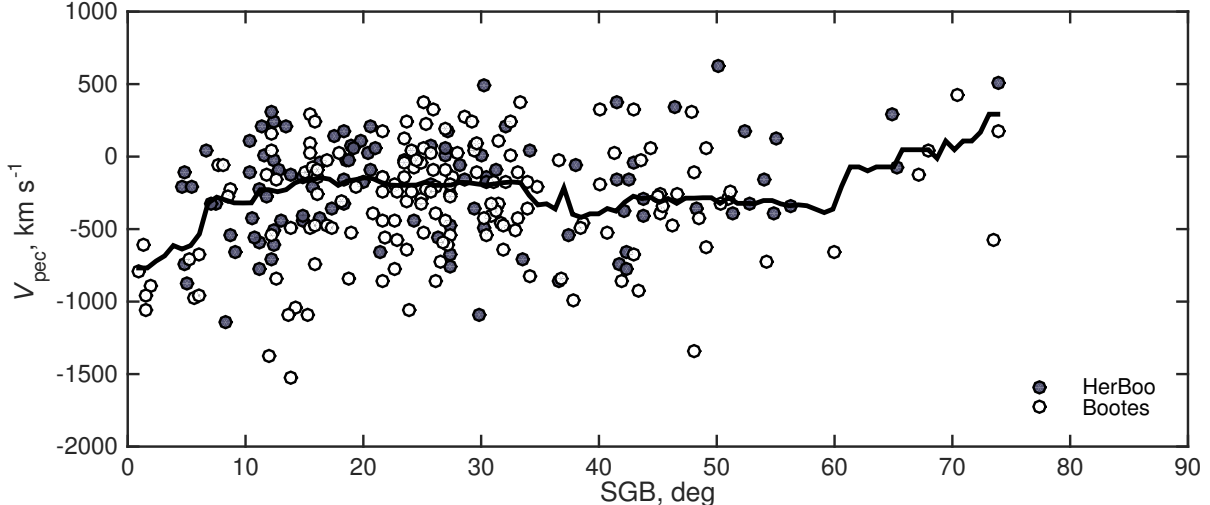


Figure 5: Peculiar velocity of the Hercules–Bootes (filled circles) and Bootes strip galaxies (open circles) depending on the supergalactic latitude. The broken line corresponds to a running median with a 2.5 window.

the flow to Virgo proves to be comparable with the virial dispersion of the cluster velocities $\sigma_V \simeq 650 \text{ km s}^{-1}$.

On the other side of the diagram at $\text{SGB} > 60^\circ$ the statistics of the peculiar velocity data is poor. Nevertheless, there is a tendency of growth of the galaxy median velocity to the region of positive values. The interpretation of this effect depends on the model assumptions on the structure and kinematics of the Local Void. If its center is located at the distance of $D_c \simeq 10 \text{ Mpc}$ [30] at $\text{SGB}_c = +77^\circ$, then the galaxies with a typical distance of $D \simeq 26 \text{ Mpc}$ around the expanding void will have a positive component of the line of sight peculiar velocity. However, the real configuration of the Local Void according to the data of [31] looks more complicated. According to these authors, the Local Void is a chain of empty volumes, which, meandering like a horseshoe, covers both the Local Volume and the Virgo cluster.

Rizzi et al. [32] have recently measured with high accuracy the *rgb*-distances to two close dwarf galaxies located not far from the direction to the center of the Local Void: KK246 ($D = 6.95 \text{ Mpc}$, $\text{SGB} = +40^\circ$), as well as ALFAZOA1952+1428 ($D = 8.39 \text{ Mpc}$, $\text{SGB} = +76^\circ$).

The galaxies have an average peculiar velocity of $-90 \pm 24 \text{ km s}^{-1}$. Given the recession velocity of the Milky Way itself from the center of the Local Void of about 230 km s^{-1} this corresponds to the recession velocity of these galaxies from the center of the void of about 320 km s^{-1} . Therefore, four different sets of observational data ([28, 30, 32], this article) on peculiar velocities of galaxies in the vicinity of the nearest void show that the walls of the void move outward from its center at a characteristic velocity of several hundred km s^{-1} .

5 Discussion

As it was repeatedly noted (see [9, 11]), the total virial mass of groups and clusters in the Local Universe with a diameter of about 100 Mpc is only 8–10% of the critical density, which is about 3 times smaller than the global density of dark matter, $\Omega_m = 0.26 \pm 0.02$. A significant enlargement of the observational base thanks to the recent optical and HI sky surveys left this contradiction almost unchanged. In this regard, it is useful to consider how the problem of missing dark matter looks like based on the data for various regions of the Local Supercluster.

Table 4 presents the main characteristics of the three regions of the sky we have studied: Leo–Cancer, the Bootes strip and Hercules–Bootes, located outside the plane of the Local Supercluster, which is laden with the projection effects. The first three lines of the table contain: the area of each region in square degrees, the maximum velocity, up to which the galaxies were considered, and the volume of each region in Mpc^3 at $H_0 = 73 \text{ km s}^{-1} \text{ Mpc}^{-1}$. The following two lines (4 and 5) contain the number of galaxies in these zones with measured radial velocities (N_V) and distances (N_D). As shown in line 6, the number densities of galaxies with measured velocities are approximately the same in the Leo–Cancer and Bootes regions, while in the Hercules–Bootes zone this density is significantly lower than in the others. The number of groups and pairs of galaxies (line 7) varies significantly from zone to zone, while the least dense area, Hercules–Bootes contains an increased number of pair systems consisting of low-luminosity galaxies. The relative number of single (non-clustered) galaxies (line 8) makes up about a half in each region, along with that, the field popula-

Table 4: Comparative properties of the three studied sky regions

Parameter	Leo–Cancer	Bootes strip	Hercules–Bootes
Sky area, sq.deg.	1477	1121	2447
$V_{\text{LG}}^{\text{max}}, \text{km s}^{-1}$	2000	2000	2500
Volume, Mpc^3	3084	2337	9975
N_V	543	361	412
N_D	290	161	181
Number density, Mpc^{-3}	0.176	0.154	0.042
$N(\text{groups+pairs})$	23+20	13+11	17+29
Fraction of isolated	0.51	0.44	0.50
$\sum M_{\text{syst}}, 10^{12} M_{\odot}$	3.50	2.63	2.62
$\rho_{\text{syst}}^*/\langle\rho^*\rangle$	2.47	2.45	0.57
$\sum M_p, 10^{13} M_{\odot}$	9.10	8.80	9.58
$\sum M_p / \sum M^*$	26	33	37

tion is dominated by dwarf galaxies. Line 9 shows the total stellar mass of galaxy members in systems of different multiplicity. Line 10 contains the value of stellar density, expressed in relation to the average cosmic density $\langle\rho^*\rangle = \langle j_K \rangle = 4.3 \times 10^8 M_{\odot} \text{Mpc}^{-3}$ according to [33] at $M^*/L_K = M_{\odot}/L_{\odot}$ [34]. As we can see, the Leo–Cancer and Bootes regions have the average stellar density 2.5 times larger than the global density, and the Hercules–Bootes region is located lower than the level of average cosmic density. The last two lines present: the total virial (projected) mass of all groups and pairs, as well as its relation to the stellar mass sum of these systems. Note that the $\sum M_p / \sum M^*$ ratio varies in a small range from 26 to 37, despite significant differences in the average stellar density from one area to another.

Given the global average stellar matter density of $\langle\rho^*\rangle = 4.3 \times 10^8 M_{\odot} \text{Mpc}^{-3}$, which is currently known with the error of about 30%, a dimensionless ratio of critical matter density to stellar density amounts to $\rho_c / \langle\rho^*\rangle = 350 \pm 100$ [35]. The observed values of $\sum M_p / \sum M^*$ in the three considered regions prove to be an order of magnitude smaller than the critical ratio.

Note that we did not take into account single non-clustered galaxies, which account for about a half of the total number of galaxies in each region. However, additional analysis shows that their contribution in the total stellar mass does not exceed 20%, since the majority of field galaxies have a low luminosity. In addition, single galaxies with their dark haloes contribute to both the denominator and the numerator of the M_{DM}/M^* ratio. This is why accounting for single galaxies can not significantly affect the values presented in the last row of Table 4. It is important to emphasize that the value of $M_{\text{DM}}/M^* \simeq 30$ is typical of the dark haloes of the Milky Way, M31, M81 and other brightest galaxies of the Local Volume [25]. Therefore, the observed lack of virial mass

in the nearby systems of galaxies is still an actual problem for the cosmology of the Local Universe.

Acknowledgments

In this paper we used the NASA Extragalactic Database (NED) and HyperLEDA database, as well as the HIPASS, ALFALFA and SDSS sky survey data. IDK and OGK are grateful to the Russian Science Foundation for the support (grant no. 14–02–00965).

References

- [1] K. N. Abazajian, J. K. Adelman-McCarthy, M. A. Agüeros, et al., *Astrophys. J. Suppl.* **182**, 543 (2009).
- [2] B. S. Koribalski, L. Staveley-Smith, V. A. Kilborn, et al., *Astronom. J.* **128**, 16 (2004).
- [3] O. I. Wong, E. V. Ryan-Weber, D. A. Garcia-Appadoo, et al., *Monthly Notices Roy. Astronom. Soc.* **371**, 1855 (2006).
- [4] L. Staveley-Smith, R. C. Kraan-Korteweg, A. C. Schröder, et al., *Astronom. J.* **151**, 52 (2016).
- [5] R. Giovanelli, M. P. Haynes, B. R. Kent, et al., *Astronom. J.* **130**, 2598 (2005).
- [6] M. P. Haynes, R. Giovanelli, A. M. Martin, et al., *Astronom. J.* **142**, 170 (2011).
- [7] I. D. Karachentsev and D. I. Makarov, *Astrophysical Bulletin* **63**, 299 (2008).
- [8] D. I. Makarov and I. D. Karachentsev, *Astrophysical Bulletin* **64**, 24 (2009).
- [9] D. Makarov and I. Karachentsev, *Monthly Notices Roy. Astronom. Soc.* **412**, 2498 (2011).

- [10] N. A. Bahcall and A. Kulier, *Monthly Notices Roy. Astronom. Soc.* **439**, 2505 (2014).
- [11] I. D. Karachentsev, *Astrophysical Bulletin* **67**, 123 (2012).
- [12] I. D. Karachentsev, O. G. Nasonova, and H. M. Courtois, *Astrophys. J.* **743**, 123 (2011).
- [13] I. D. Karachentsev, O. G. Nasonova, and H. M. Courtois, *Monthly Notices Roy. Astronom. Soc.* **429**, 2264 (2013).
- [14] I. D. Karachentsev and O. G. Nasonova, *Monthly Notices Roy. Astronom. Soc.* **429**, 2677 (2013).
- [15] I. D. Karachentsev, V. E. Karachentseva, and O. G. Nasonova, *Astrophysics* **57**, 457 (2014).
- [16] I. D. Karachentsev, O. G. Nasonova, and V. E. Karachentseva, *Astrophysical Bulletin* **70**, 1 (2015).
- [17] D. Makarov, P. Prugniel, N. Terekhova, et al., *Astronom. and Astrophys.* **570**, A13 (2014).
- [18] E. F. Schlafly and D. P. Finkbeiner, *Astrophys. J.* **737**, 103 (2011).
- [19] M. A. W. Verheijen and R. Sancisi, *Astronom. and Astrophys.* **370**, 765 (2001).
- [20] J. L. Tonry, A. Dressler, J. P. Blakeslee, et al., *Astrophys. J.* **546**, 681 (2001).
- [21] R. B. Tully and J. R. Fisher, *Astronom. and Astrophys.* **54**, 661 (1977).
- [22] R. B. Tully, L. Rizzi, E. J. Shaya, et al., *Astronom. J.* **138**, 323 (2009).
- [23] R. B. Tully, H. M. Courtois, A. E. Dolphin, et al., *Astronom. J.* **146**, 86 (2013).
- [24] R. B. Tully, H. M. Courtois, and J. G. Sorce, *Astronom. J.* **152**, 50 (2016).
- [25] I. D. Karachentsev and Y. N. Kudrya, *Astronom. J.* **148**, 50 (2014).
- [26] R. B. Tully and N. Trentham, *Astronom. J.* **135**, 1488 (2008).
- [27] S. Kim, S.-C. Rey, M. Bureau, et al., *Astrophys. J.* **833**, 207 (2016).
- [28] R. B. Tully, E. J. Shaya, I. D. Karachentsev, et al., *Astrophys. J.* **676**, 184 (2008).
- [29] A. V. Tikhonov and I. D. Karachentsev, *Astrophys. J.* **653**, 969 (2006).
- [30] O. G. Nasonova and I. D. Karachentsev, *Astrophysics* **54**, 1 (2011).
- [31] A. A. Elyiv, I. D. Karachentsev, V. E. Karachentseva, et al., *Astrophysical Bulletin* **68**, 1 (2013).
- [32] L. Rizzi, R. B. Tully, E. J. Shaya, et al., *Astrophys. J.* **835**, 78 (2017).
- [33] D. H. Jones, B. A. Peterson, M. Colless, and W. Saunders, *Monthly Notices Roy. Astronom. Soc.* **369**, 25 (2006).
- [34] E. F. Bell, D. H. McIntosh, N. Katz, and M. D. Weinberg, *Astrophys. J. Suppl.* **149**, 289 (2003).
- [35] M. Fukugita and P. J. E. Peebles, *Astrophys. J.* **616**, 643 (2004).

Translated by A. Zyazeva